ChemComm

Reversible structural rearrangement of π-expanded cyclooctatetraene upon two-fold reduction with alkali metals

Journal:	*ChemComm*
Manuscript ID	CC-COM-01-2022-000218.R2
Article Type:	Communication

COMMUNICATION

Reversible structural rearrangement of π-expanded cyclooctatetraene upon two-fold reduction with alkali metals

Received 00th January 20xx,
Accepted 00th January 20xx

DOI: 10.1039/x0xx00000x

Zheng Zhou,[a,b] Yikun Zhu,[a] Zheng Wei,[a] John Bergner,[c,d] Christian Neiß,[e] Susanne Doloczki,[f] Andreas Görling,[e] Milan Kivala,[*c,d] and Marina A. Petrukhina[*a]

The chemical reduction of a π-expanded COT derivative, octaphenyltetrabenzocyclooctatetraene (1), with lithium or sodium metals in thee presence of secondary ligands affords a new doubly-reduced product ($\mathbf{1}_{TR}^{2-}$). The X-ray diffraction study revealed a reductive core rearrangement accompanied by the formation of a single C–C bond and severe twist of the central tetraphenylene core. The reversibility of two-electron reduction and core transformation are further confirmed by NMR spectroscopy and DFT calculations.

The tub-shaped 8π-electron non-aromatic framework of cyclooctatetraene (COT) with its conformational flexibility represents a versatile construction building block for the development of stimuli responsive materials.[1-3] Hence, COT derivatives were shown to undergo a tub-to-tub inversion[4, 5] and to planarize upon photoexcitation[6] which was employed in photoresponsive liquid crystals and molecular viscosity probes.[7] Moreover, recent studies were directed toward planarization dynamics of functionalized COTs and their excited-state aromaticity.[8, 9] More importantly, the COT moiety shows pronounced responsivity in redox processes leading to geometry changes, bond shifting, and valence isomerization. Both two-electron oxidation and reduction lead to a planar conformation as a result of aromaticity gain in the COT^{2+} dication[10, 11] and COT^{2-} dianion,[12, 13] respectively. Furthermore, various valence isomerizations of cationic and anionic states leading to a range of electronically and structurally unusual species were described in literature.[14-17] However, most of these interesting processes were irreversible, which disqualifies them from potential application in stimuli-responsive materials. The appealing exception is the electron-rich π-expanded COT derivative, octamethoxytetraphenylene (OMT), capable of undergoing a reversible structural rearrangement upon two-electron chemical and electrochemical oxidation.[18] The process is accompanied by a dramatic color change from yellow to red which makes it interesting in the context of electrochromism.

Within our research efforts directed toward the development of new types of electron acceptors based on polycyclic aromatic hydrocarbons (PAHs) with nonbenzenoid moieties,[19, 20] we have recently reported the chemical reduction of π-expanded COT derivative, octaphenyltetrabenzo-cyclooctatetraene (OPTBCOT, **1**, Scheme 1). Remarkably, reaction of **1** with excess lithium metal afforded a coordinatively stabilized tetraanion instead of the planarized aromatic dianion.[21]

In this work, we aimed to access the doubly-reduced state of **1** as its highly twisted π-expanded framework is expected to prevent the planarization of the core upon two-fold reduction and thus enable unusual reactivity or structural rearrangement. In order to facilitate the formation of "naked" carbanions without metal binding influence, we selected light alkali metals and strongly coordinating secondary ligands such as [2.2.2]cryptand and 18-crown-6 ether.

We were pleased to discover that under the conditions used (Scheme 1), the reaction of **1** with lithium and sodium metals in THF resulted in a two-electron reduction. The X-ray crystallographic investigation revealed a dramatic skeletal core

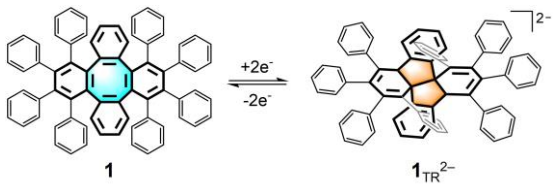

Scheme 1 Depiction of the redox process of **1**.

[a] *Department of Chemistry, University at Albany, State University of New York, Albany, NY 12222, USA. E-mail: mpetrukhina@albany.edu*
[b] *School of Materials Science and Engineering, Tongji University, Shanghai 201804, China*
[c] *Organisch-Chemisches Institut, Ruprecht-Karls-Universität Heidelberg, 69120 Heidelberg, Germany. E-mail: milan.kivala@oci.uni-heidelberg.de*
[d] *Centre for Advanced Materials, Ruprecht-Karls-Universität Heidelberg, 69120 Heidelberg, Germany*
[e] *Department of Chemistry and Pharmacy, Chair of Theoretical Chemistry Friedrich-Alexander-Universität, 91058 Erlangen, Germany*
[f] *Department of Chemistry and Pharmacy, Chair of Organic Chemistry I Friedrich-Alexander-Universität, 91058 Erlangen, Germany*
Electronic Supplementary Information (ESI) available: Details of preparation and X-ray diffraction study. CCDC 2117102-2117103. For ESI and crystallographic data in CIF or other electronic format see DOI:10.1039/x0xx00000x

rearrangement towards a new dianion, $\mathbf{1}_{TR}^{2-}$, which was not observed prior to this work.

The chemical reduction of **1** with Li or Na metal in the presence of [2.2.2]cryptand and 18-crown-6 ether (Scheme 2) is accompanied by a pronounced color change and proceeds through two steps, which is different compared to the reduction observed in THF only.[21] The reaction solution color quickly turns blue followed by purple (483 and 576 nm) which is indicative of the formation of doubly-reduced product according to the UV-Vis spectroscopy (Figs. S1–S4). By slow diffusion of freshly distilled hexanes to the THF solution, the resulting products have been isolated as black plate-shaped crystals in moderate yield. The X-ray diffraction confirmed the formation of two solvent-separated ion products (SSIP) with lithium and sodium counterions, namely $[\{Li^+([2.2.2]cryptand)\}_2(\mathbf{1}_{TR}^{2-})]$ (**2**, crystallized with two interstitial THF molecules as **2**·2THF) and $[\{Na^+(18\text{-crown-6})(THF)_2\}_2(\mathbf{1}_{TR}^{2-})]$ (**3**, crystallized as **3**·3THF). The latter contains two independent dianions (Fig. S25), and only one is discussed below due to their similarity.

In the crystal structure of **2** (Fig. 1a), each Li^+ ion is fully entrapped by a [2.2.2]cryptand molecule, and both $[Li^+([2.2.2]cryptand)]$ cations remain solvent-separated from the $\mathbf{1}_{TR}^{2-}$ dianion. The Li···O (1.998(15)–2.399(15) Å) and Li···N (2.229(15)/2.310(15) Å) distances are close to the values reported in the literature.[22-23] Notably, the core transformation is observed to form the $\mathbf{1}_{TR}^{2-}$ anion. Specifically, the central eight-membered ring is transformed into two fused five-membered rings with a new C–C bond of 1.619(11) Å between the C51 and C59 atoms (Fig. 1b).

In the crystal structure of **3** (Fig. 2a), each Na^+ ion is hexa-coordinated to one 18-crown-6 ether ($Na\cdots O_{crown}$, 2.358(13)–2.974(15) Å) and capped by two THF molecules ($Na\cdots O_{THF}$, 2.309(16)–2.373(15) Å),[24, 25] and both cations are also solvent-separated from the $\mathbf{1}_{TR}^{2-}$ dianion. Similarly, two fused five-membered rings are formed with the C51–C59 bond length of 1.545(9) Å. In comparison to that in OMT^{2+} (1.560(10) Å),[18] the newly formed C–C bond is slightly shorter in **3** but longer in **2**, illustrating sufficient flexibility of the central core. This bond is also comparable with the single C–C bonds ranging from 1.560(8) Å to 1.588(5) Å observed in the σ-coupled dimers of bowl-shaped radicals.[26, 27] As expected, the use of strongly-coordinating secondary ligands facilitated the formation of "naked" $\mathbf{1}_{TR}^{2-}$ anions in **2** and **3**, thus showing that the core transformation is not induced by direct metal coordination and stems from the two-electron acquisition.

In the solid-state structure of **2**, the 1D columns are formed through C–H···π interactions between the $\mathbf{1}_{TR}^{2-}$ anions and the cationic $\{Li^+([2.2.2]cryptand)\}$ moieties (Fig. S28a), with the shortest contacts ranging over 2.581(11)–2.806(11) Å (Fig. S29). In contrast, a 3D network is observed in the solid-state structure of **3** (Fig. S28b) with multiple C–H···π contacts (2.483(9)–2.786(9) Å) between the $\mathbf{1}_{TR}^{2-}$ anions and the $\{Na^+(18\text{-crown-6})(THF)_2\}$ cationic moieties (Fig. S30).

The core rearrangement upon two-fold reduction is also accompanied by the twist of the central tetraphenylene part of $\mathbf{1}_{TR}^{2-}$ (Scheme 1). In **1**, the saddle-shaped conformation allows rings A and B to be on one side of the eight-membered ring with the torsion and dihedral angles of 19.8° and 70.7°, respectively (Fig. 3). In contrast, these two rings in the $\mathbf{1}_{TR}^{2-}$ anion become twisted, with the torsion and dihedral angles of 85.5° and 83.1° in **2** (71.0° and 80.8° in **3**). Moreover, the aromaticity of rings A and B has decreased, as revealed by the changes in bond lengths and ring planarity (Tables S2 and S3). In **1**, the average of bond

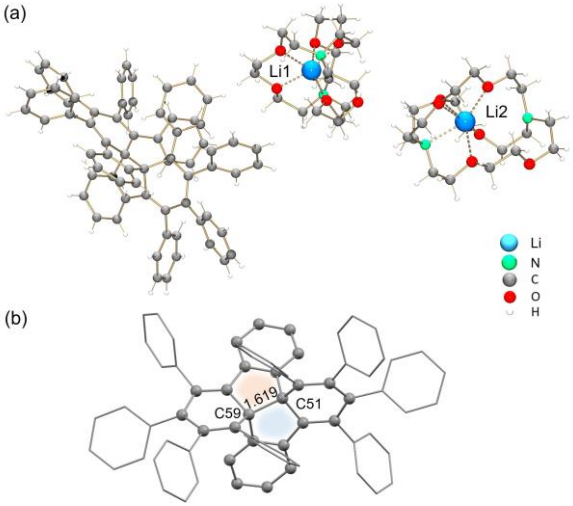

Fig. 1 (a) Crystal structure of **2** (ball-and-stick model) and (b) new $\mathbf{1}_{TR}^{2-}$ core (mixed model, H-atoms are removed).

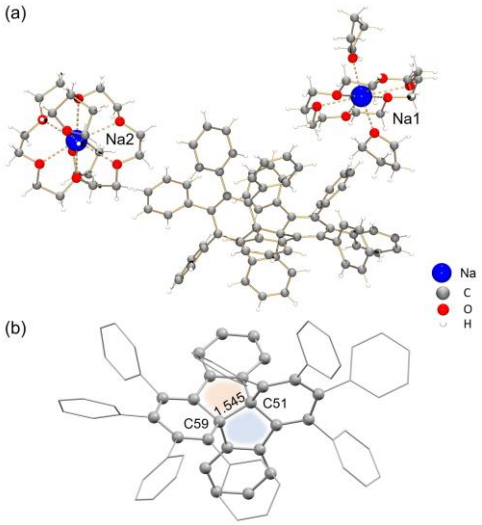

Fig. 2 (a) Crystal structure of **3** (ball-and-stick model) and (b) new $\mathbf{1}_{TR}^{2-}$ core (mixed model, H-atoms are removed).

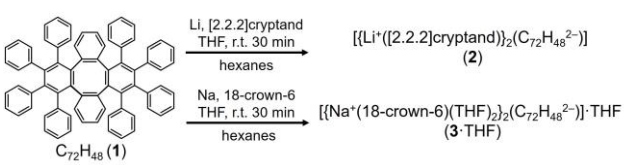

Scheme 2 Chemical reduction of **1** with Li and Na metals in the presence of secondary ligands.

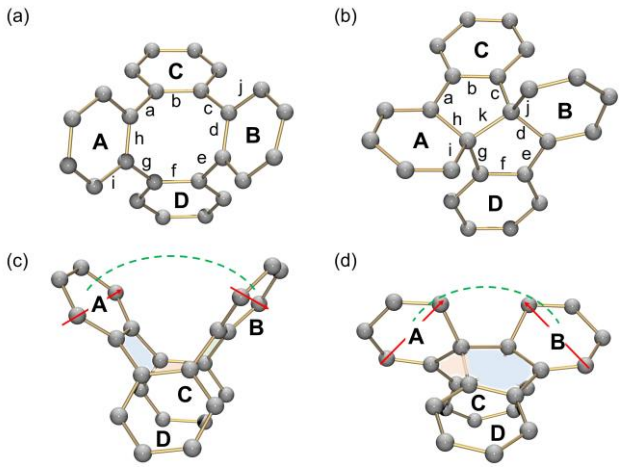

Fig. 3 Face and side views of the tetraphenylene core in (a) (c) **1** and (b) (d) $\mathbf{1}_{TR}^{2-}$ in **2**, ball-and-stick models, along with the labeling of selected C–C bonds and calculation of torsion (red) and dihedral (green) angles.

lengths at d, h, i, j of 1.407(4) Å is in the range of aromatic C–C bonds (Fig. 4). In contrast, the average values of these bonds in **2** and **3** are increased to 1.544(11) Å and 1.544(10) Å, respectively. According to the planarity calculations (Table S2), the distances out of plane for rings A and B are much larger in **2** and **3** compared to those in the neutral state, which is indicative of their reduced planarity or aromaticity upon core transformation.

Furthermore, the carbon framework shows structural flexibility that can be demonstrated by comparing the geometry of two $\mathbf{1}_{TR}^{2-}$ anions in **2** and **3**. In **3**, the dihedral angles of rings A and B with their phenyl rings range from 48.2° to 86.6° (Fig. 1b). In **2**, those angles fall in a broader range (44.0°–88.7°, Fig. 2b). The core transformation after the two-electron uptake leads to the charge distribution change of the external phenyl rings, as demonstrated by a wider aromatic signal range detected by the ^{1}H NMR spectroscopy (Figs. S5–S11). Moreover, the NMR data point out the reversibility of the observed core transformation. In the ^{13}C NMR spectrum of neutral **1** (Fig. 5a), the signals of C51 and C59 appear at 139.4 ppm, comparable to the reported value.[28] Upon two-fold reduction, the corresponding peak is shifted to 68.6 ppm in $\mathbf{1}_{TR}^{2-}$ (Fig. 5b), which is indicative of the formation of the sp^3-hybridized C-atoms at the coupling site. Upon brief exposure of the reduced product to air, this signal is shifted back to the aromatic region (139.4 ppm, Fig. 5c), suggesting that both the redox reaction and core transformation are reversible.

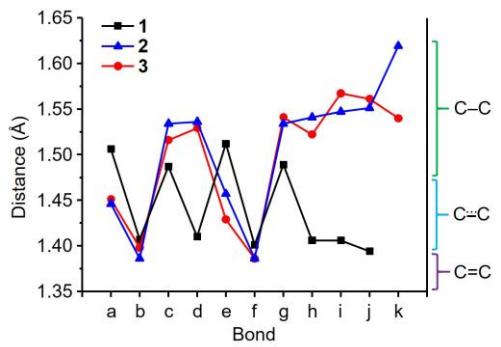

Fig. 4 Comparison of selected C–C bond lengths in **1** and $\mathbf{1}_{TR}^{2-}$ in **2** and **3**.

To get deeper insight into the reduction and rearrangement reactions we carried out DFT calculations where solvent effects have been included via a polarizable continuum (see the ESI for technical details). Using the experimental vaporization energy of solid lithium, we calculated the reaction energy of the reduction with lithium according to:

$$2\text{Li(solid)} + \mathbf{1} + 2[2.2.2]\text{cryptand} \rightarrow \mathbf{1}^{2-} + 2\{\text{Li}^{+}([2.2.2]\text{cryptand})\}$$

We found that the formation of the dianionic species $\mathbf{1}^{2-}$ is nearly energy neutral with $\Delta H° = -3$ kcal/mol. Including entropic effects, the reduction is slightly endergonic with $\Delta G° = +7$ kcal/mol (Note that this is approximately the order of magnitude of the expected error of the DFT calculations). In fact, the addition of two electrons is experimentally reversible (Scheme 1), as the $\mathbf{1}_{TR}^{2-}$ anion can be oxidized back to the neutral state according to the NMR and DART-MS spectroscopic investigations (Figs. S19–S23).

The charge distribution in $\mathbf{1}^{2-}$ reveals that the negative charge is essentially located at the tetraphenylene core (Fig. S32). The core transformation $\mathbf{1}^{2-} \rightarrow \mathbf{1}_{TR}^{2-}$ introduces a new C–C single bond (calculated bond length: 1.61 Å) which is confirmed by a Mayer bond order[29, 30] of 1.1 between the two C-atoms. After the core rearrangement, the negative charge is still located on the core of the molecule (Figs. 6 and S33). The free energy change of the core transformation is also quite small: we calculate $\Delta G° = -1$ kcal/mol. We note in passing that the core transformation of the monoanion, i.e. $\mathbf{1}^{-}$, is in contrast clearly endergonic with $\Delta G° = +24$ kcal/mol.

To assess the activation barrier of the dianion transformation we tried to compute its transition state. However, due to the high flexibility of $\mathbf{1}^{2-}$, we were not able to locate the transition state accurately. Therefore, we also

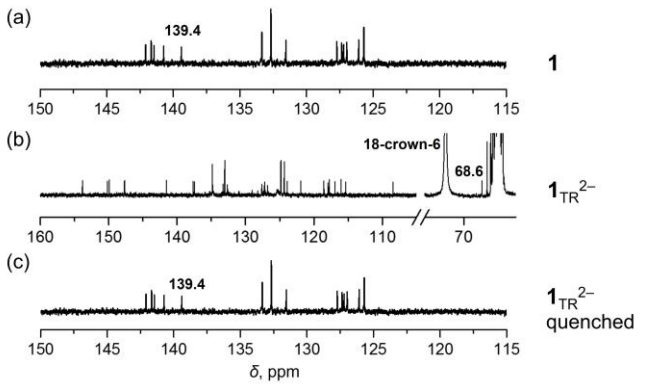

Fig. 5 ^{13}C NMR (126 MHz) spectra of (a) **1**, (b) *in situ* generated $\mathbf{1}_{TR}^{2-}$ with Na and 18-crown-6 ether, and (c) its quenched product at 25 °C in THF-d_8, aromatic regions.

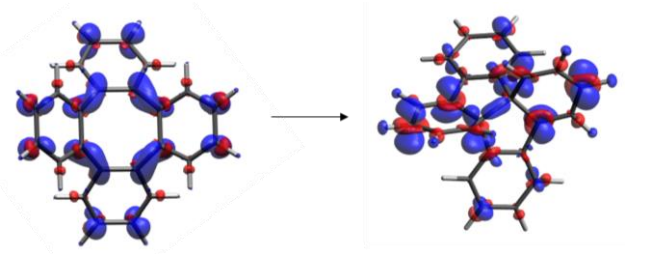

Fig. 6 Structural and charge rearrangement upon transformation of $\mathbf{1a}^{2-}$ (= $\mathbf{1}^{2-}$ without phenyl substituents). Blue: Increase of electron density, red: decrease of electron density with respect to the neutral species. Iso-surfaces plotted at 0.004 e/Bohr^{-3}.

considered the molecule with the attached phenyl rings replaced by H-atoms, i.e. the molecule representing the tetraphenylene core (denoted **1a** in the following, see Fig. 6. The free energy change of –5 kcal/mol upon core transformation of $\mathbf{1a}^{2-}$ is similar to that of $\mathbf{1}^{2-}$ confirming that the phenyl rings of $\mathbf{1}^{2-}$ are largely electronically decoupled from the tetraphenylene core. The back transformation $\mathbf{1a}_{TR}^{2-} \rightarrow \mathbf{1a}^{2-}$ exhibits a single transition state with $\Delta G^{\neq}$ = +17 kcal/mol (imaginary vibrational frequency $\nu^{\neq}$ = 161i cm^{-1}) indicating a reversible reaction at room temperature. From a mechanistic point of view, the rearrangement is an orbital-symmetry allowed electrocyclic reaction, which explains the low activation barrier. Fig. S34 shows the HOMO of $\mathbf{1a}^{2-}$ in course of the cyclization.

In summary, the controlled chemical reduction of large and contorted OPTBCOT (**1**) with different alkali metals in the presence of secondary ligands has been investigated. In contrast to the previously reported tetra-reduced product of **1**,[21] the uptake of two electrons is accompanied by an unusual transformation of the negatively charged core, which has been confirmed by X-ray crystallography. Notably, the new dianion with a more twisted COT moiety has been formed rather than the expected planarized aromatic core. Moreover, the reduction and core transformation have been proved to be reversible at room temperature using a combination of NMR spectroscopy and DFT calculations. To the best of our knowledge, such reductive rearrangement of a π-expanded COT derivative has not been observed before and as such it opens new complementary avenues towards redox-controlled molecular switches.

Financial support from the U. S. National Science Foundation, CHE-2003411, is gratefully acknowledged by M. A. P. The generous funding by the Deutsche Forschungsgemeinschaft (DFG) – Project number 182849149 – SFB 953 is acknowledged.

Conflicts of interest

There are no conflicts to declare.

Notes and references

1. L. A. Paquette, *Tetrahedron*, 1975, **31**, 2855-2883.
2. M. J. Marsella, *Acc. Chem. Res.*, 2002, **35**, 944-951.
3. R. D. Kennedy, D. Lloyd and H. McNab, *J. Chem. Soc., Perkin Trans. 1*, 2002, 1601-1621.
4. J. L. Andrés, O. Castaño, A. Morreale, R. Palmeiro and R. Gomperts, *J. Phys. Chem.*, 1998, **108**, 203-207.
5. T. Nishinaga, T. Ohmae and M. Iyoda, *Symmetry*, 2010, **2**, 76-97.
6. T. Yamakado, S. Takahashi, K. Watanabe, Y. Matsumoto, A. Osuka and S. Saito, *Angew. Chem. Int. Ed.*, 2018, **57**, 5438-5443.
7. M. Hada, S. Saito, S. i. Tanaka, R. Sato, M. Yoshimura, K. Mouri, K. Matsuo, S. Yamaguchi, M. Hara, Y. Hayashi, F. Röhricht, R. Herges, Y. Shigeta, K. Onda and R. J. D. Miller, *J. Am. Chem. Soc.*, 2017, **139**, 15792-15800.
8. H. Ottosson, *Nat. Chem.*, 2012, **4**, 969-971.
9. M. Rosenberg, C. Dahlstrand, K. Kilså and H. Ottosson, *Chem. Rev.*, 2014, **114**, 5379-5425.
10. G. A. Olah, J. S. Staral and L. A. Paquette, *J. Am. Chem. Soc.*, 1976, **98**, 1267-1269.
11. G. A. Olah, J. S. Staral, G. Liang, L. A. Paquette, W. P. Melega and M. J. Carmody, *J. Am. Chem. Soc.*, 1977, **99**, 3349-3355.
12. T. J. Katz, *J. Am. Chem. Soc.*, 1960, **82**, 3784-3785.
13. T. J. Katz, *J. Am. Chem. Soc.*, 1960, **82**, 3785-3786.
14. W. E. Geiger, P. H. Rieger, C. Corbato, J. Edwin, E. Fonseca, G. A. Lane and J. M. Mevs, *J. Am. Chem. Soc.*, 1993, **115**, 2314-2323.
15. S. Kato, R. Gareyev, C. H. DePuy and V. M. Bierbaum, *J. Am. Chem. Soc.*, 1998, **120**, 5033-5042.
16. O. Castaño, L.-M. Frutos, R. Palmeiro, R. Notario, J.-L. Andrés, R. Gomperts, L. Blancafort and M. A. Robb, *Angew. Chem. Int. Ed.*, 2000, **39**, 2095-2097.
17. S. Nobusue, K. Fujita and Y. Tobe, *Org. Lett.*, 2017, **19**, 3227-3230.
18. R. Rathore, P. Le Magueres, S. V. Lindeman and J. K. Kochi, *Angew. Chem. Int. Ed. Engl.*, 2000, **39**, 809-812.
19. Y. Zhu, Z. Zhou, Z. Wei and M. A. Petrukhina, *Organometallics*, 2020, **39**, 4688-4695.
20. Y. Zhang, Y. Zhu, D. Lan, S. H. Pun, Z. Zhou, Z. Wei, Y. Wang, H. K. Lee, C. Lin, J. Wang, M. A. Petrukhina, Q. Li and Q. Miao, *J. Am. Chem. Soc.*, 2021, **143**, 5231-5238.
21. Z. Zhou, Y. Zhu, Z. Wei, J. Bergner, C. Neiß, S. Doloczki, A. Görling, M. Kivala and M. A. Petrukhina, *Angew. Chem. Int. Ed.*, 2020, **60**, 3510-3514.
22. A. V. Zabula, A. S. Filatov, S. N. Spisak, A. Yu. Rogachev and M. A. Petrukhina, *Science*, 2011, **333**, 1008-1011.
23. A. S. Filatov, A. V. Zabula, S. N. Spisak, A. Yu. Rogachev and M. A. Petrukhina, *Angew. Chem. Int. Ed.*, 2014, **53**, 140-145.
24. Z. Zhou, Z. Wei, Y. Tokimaru, S. Ito, K. Nozaki and M. A. Petrukhina, *Angew. Chem. Int. Ed.*, 2019, **58**, 12107-12111.
25. Z. Zhou, X.-Y. Wang, Z. Wei, K. Müllen and M. A. Petrukhina, *Angew. Chem. Int. Ed.*, 2019, **58**, 14969-14973.
26. S. N. Spisak, A. V. Zabula, M. Alkan, A. S. Filatov, A. Yu. Rogachev and M. A. Petrukhina, *Angew. Chem. Int. Ed.*, 2018, **57**, 6171-6175.
27. A. Yu. Rogachev, Y. Zhu, Z. Zhou, S. Liu, Z. Wei and M. A. Petrukhina, *Org. Chem. Front.*, 2020, **7**, 3591-3598.
28. M. Müller, V. S. Iyer, C. Kübel, V. Enkelmann and K. Müllen, *Angew. Chem. In. Ed Engl.*, 1997, **36**, 1607-1610.
29. I. Mayer, *Int. J. Quantum Chem*, 1986, **29**, 73-84.
30. A. J. Bridgeman, G. Cavigliasso, L. R. Ireland and J. Rothery, *J. Chem. Soc., Dalton Trans.*, 2001, 2095-2108.